Published in final edited form as:

Macromolecules. 2017 ; 50: . doi:10.1021/acs.macromol.7b01717.

Energy-Renormalization for Achieving Temperature Transferable Coarse-Graining of Polymer Dynamics

Wenjie Xia[#⊥,†,¶], **Jake Song**[#‡,#], **Cheol Jeong**[⊥], **David D. Hsu**[§], **Frederick R. Phelan Jr.**[⊥], **Jack F. Douglas**[*,⊥], and **Sinan Keten**[*,§,†]

[⊥] Materials Science & Engineering Division, National Institute of Standards and Technology, Gaithersburg, Maryland 20899, United States

[†] Department of Civil & Environmental Engineering, Northwestern University, 2145 Sheridan Road, Evanston, Illinois 60208-3109, United States

[‡] Department of Materials Science & Engineering, Northwestern University, 2145 Sheridan Road, Evanston, Illinois 60208-3109, United States

[§] Department of Mechanical Engineering, Northwestern University, 2145 Sheridan Road, Evanston, Illinois 60208-3109, United States

[¶] Center for Hierarchical Materials Design, Northwestern University, Evanston, Illinois 60208-3109, United States

[#] These authors contributed equally to this work.

Abstract

The bottom-up prediction of the properties of polymeric materials based on molecular dynamics simulation is a major challenge in soft matter physics. Coarse-grained (CG) models are often employed to access greater spatiotemporal scales required for many applications, but these models normally experience significantly altered thermodynamics and highly accelerated dynamics due to the reduced number of degrees of freedom upon coarse-graining. While CG models can be calibrated to meet certain properties at particular state points, there is unfortunately no *temperature transferable and chemically specific* coarse-graining method that allows for modeling of polymer dynamics over a wide temperature range. Here, we pragmatically address this problem by "correcting" for deviations in activation free energies that occur upon coarse-graining the dynamics of a model polymeric material (polystyrene). In particular, we propose a new strategy based on concepts drawn from the Adam−Gibbs (AG) theory of glass formation. Namely we renormalize the cohesive interaction strength and effective interaction length-scale parameters to modify the activation free energy. We show that this energy-renormalization method for CG modeling allows accurate prediction of atomistic dynamics over the Arrhenius regime, the non-

[*]**Corresponding Authors:** (J.F.D.) jack.douglas@nist.gov., (S.K.) s-keten@northwestern.edu.
[#]Current Address: Dept. of Materials Science and Engineering, Massachusetts Institute of Technology, 77 Massachusetts Avenue, Cambridge, MA 02139, United States.

The authors declare no competing financial interest.

ASSOCIATED CONTENT
S Supporting Information
The Supporting Information is available free of charge on the ACS Publications website at DOI: 10.1021/acs.macromol.7b01717.
Additional information on the all-atomistic and coarsegrained modeling details and analysis (PDF)

Arrhenius regime of glass formation, and even the non-equilibrium glassy regime, thus allowing for the predictive modeling of dynamic properties of polymer over the entire range of glass formation. Our work provides a practical scheme for establishing temperature transferable coarse-grained models for predicting and designing the properties of polymeric materials.

GRAPHICAL ABSTRACT

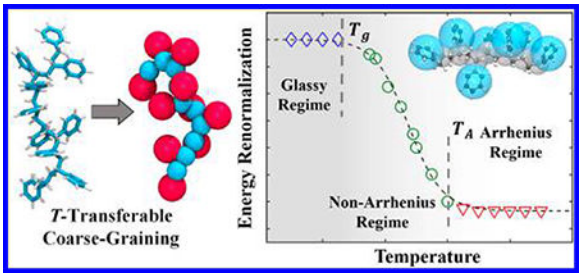

1. INTRODUCTION

Glass-forming (GF) polymer liquids have diverse applications in structural components, electronics, and biomaterials. However, the bottom-up prediction of the dynamical behavior of glasses at arbitrary temperatures remains a major challenge.[1–3] In accord with recent advances in computational materials science, there has been growing interest in applying all-atomistic (AA) modeling techniques to link the molecular features of GF polymers to their dynamical properties.[4–6] However, the steep increase in viscosity and relaxation times of GF liquids upon vitrification greatly limits what can be learned from AA simulations. This has necessitated modeling techniques that can access greater spatiotemporal scales while retaining chemical specificity, such as atomistically informed coarse-grained (CG) modeling.

Many of the proposed CG modeling efforts have focused on accurately reproducing the many-body potential of mean force (PMF) of a starting AA model in order to preserve the thermodynamic properties of the fluid under coarse-graining. One classic approach is to derive CG force-fields by AA probability distribution inversions, such as the inverse Boltzmann method (IBM)[4,5,7] and inverse Monte Carlo.[8] Other means to achieve this include the multiscale coarsegraining (MS-CG) approach,[9–12] which minimizes a forcematching functional of the CG force-field, and the relative entropy method,[13,14] which reproduces the configurational entropy s_c of the CG bead sites present in the AA model through a minimization effort (on their relative entropy difference). Despite the success of these approaches in representing key structural features and thermodynamics for CG modeling, it is generally observed that the resulting CG models exhibit an accelerated dynamics and softer mechanical responses relative to their AA counterpart.[6,7,15] This occurs mainly because of the reduced degree of freedoms associated with s_c under coarse-graining, which can be viewed as reducing fluctuating and frictional forces associated with lost fine atomistic details as pointed out in specific statistical mechanical models and theories.[16–19] The central role of s_c in the collective dynamics of GF systems has been emphasized by Adam and Gibbs (AG),[20] who introduced a highly successful model of the how the

segmental friction coefficient of polymers in the melt is related to the configurational entropy s_c. On the basis of the AG theory, it is expected that the loss of s_c due to coarse-graining inevitably causes a change in the activation free energy in the regime of incipient glass formation, where molecular motion becomes progressively more cooperative upon cooling.[20] The alteration of s_c under coarse-graining is then expected to lead to a serious problem in describing the dynamics of polymeric and other GF liquids, which might ultimately limit the practical value of CG modeling for polymeric materials.

Numerous methods have instead focused on accurately reproducing the AA dynamics by CG models rather than thermodynamics. Such methods emphasize the need to introduce nonconservative forces (i.e., dissipative and random forces) to the CG degrees of freedom at a given state point. These methods include the generalized Langevin equations,[19,21] dissipative particle dynamics (DPD),[22–25] dynamic relative entropy (formulated in terms of time correlation function),[26] dynamic force-matching (using particles that mimic Langevin heat-baths),[27,28] and nonequilibrium thermodynamics (via a nonequilibrium reversible-irreversible coupling (GENERIC) formalism).[16,17] Despite the success of these approaches in reproducing AA melt dynamics at finite state points, the transferability (i.e., temperature transferability) of these methods remains a significant hurdle.[29] This is a particular challenge for the prediction of the dynamic properties of GF polymers, which characteristically exhibit a dramatic slowdown in their dynamics upon cooling.[1] A fundamental understanding of the strong temperature dependence of the GF dynamics is known to be one of the most difficult problems in condensed matter physics so that a rigorous treatment of how coarsegraining influences nonconservative forces seems to be out of question. As one might expect, the aforementioned frictional terms alone have generally failed to account for the dynamics and mechanics of cooled polymer fluids, particularly in the glassy regime where such materials are normally utilized.[15] Currently, it is rather unclear as to how to account for the temperature dependence of these dissipative terms in order to predict polymer properties as a function of temperature for use in practical applications.

In the present work, we address this fundamental problem (i.e., capturing the GF dynamics) through an alternative CG modeling strategy based on the AG theory[20] of liquid state dynamics that emphasizes the significance of the configurational entropy s_c for the dynamics of GF fluids. We also base our CG method on the general observations that changes in the enthalpy of activation by changes in molecular parameters (e.g., cohesive interactions) lead to a proportionate change in the entropy of activation, called the “entropy−enthalpy compensation” effect.[30–35] Our hypothesis is that if this effect exists under coarse-graining, it ay provide a means for predicting how the energetic parameters governing fluid dynamics become modified to compensate for the reduction in overall s_c under coarse-graining.

Here, we take advantage of the compensation effect to develop a temperature transferable CG model that covers the entire range of glass formation. Specifically, we introduce temperature-dependent renormalizations of the cohesive interaction parameter ε and length-scale parameter σ in our CG model, which are directly related to the cohesive energy of the material.[36,37] Recent simulation studies exploring the variation of ε revealed that this parameter has a large effect on the dynamics and mechanical properties of the polymers, such as the Young’s modulus E and glass-transition temperature T_g,[36,38–41] establishing the

signicance of utilizing this energetic parameter in CG model development. We demonstrate our approach on a CG model of atactic polystyrene (PS) (Figure 1a), and show that our energy-renormalization method is able to replicate the dynamics of the atomistic PS model in the CG model calculations over the entire temperature (T) range of glass formation−from the high-T Arrhenius dynamics regime to the cooled GF regime (where the dynamics is highly nonArrhenius) and the low-T glassy regime.

2. COARSE-GRAINING STRATEGY

2.1. Influence of Coarse-Graining on Activation Energies in Cooled Liquids.

Our energy-renormalization approach starts from the common observation that the dynamics of fluids at elevated temperatures is universally described by an Arrhenius activated behavior, as expected from the transition state theory developed long ago by Eyring and co-workers.[42,43] This has provided a powerful semiempirical framework for understanding observed trends in the dynamics of fluids at elevated temperatures, where relaxation times, viscosity and diffusion coefficients all exhibit an Arrhenius temperature dependence. Adam and Gibbs (AG)[20] later generalized this transition state theory framework to cooled liquids, which often exhibit a non-Arrhenius structural relaxation time τ governed by a temperature-dependent free energy of activation $\Delta G(T)$:

$$\tau = \tau_0 \exp\left(\frac{\Delta G(T)}{k_B T}\right) \quad (1)$$

where τ_0 is vibrational relaxation time and $k_B T$ is the thermal energy. The main idea behind the AG theory is that the increase in ΔG associated with segmental relaxation time and the resulting slowdown in the dynamics of complex fluids upon cooling arise from the growth of "cooperatively rearranging regions" (CRR). Specifically, AG argued that ΔG is renormalized by the factor $z(T)$, the ratio of $s_c(T)$ with its high temperature limiting value s_c^*,

$$\Delta G(T) = z(T)\Delta\mu \quad (2)$$

where $\Delta\mu$ is free energy of activation (assumed by AG to be predominantly enthalpic) in the Arrhenius relaxation regime and $z(T) \equiv \frac{s_t^*}{s_c(T)}$ (the CRR "size" in AG terminology) governs the energy barrier for non-Arrhenius relaxation, where s_c^* is the configurational entropy (density) in the high temperature Arrhenius regime. While the arguments of the original AG theory were rather heuristic in nature, their predictions have been found to be supported subsequently by a large body of evidence,[33,44,45] and we base our CG method partly on this classic model of the dynamics of GF liquids.

The accelerated dynamics of CG models relative to the atomistic counterpart is often described by an empirical scaling factor ζ ($\gg 1$) defined as the ratio of CG to AA diffusivity, i.e., $\zeta = D_{CG}/D_{AA}$.[7] Previous studies have shown that this ζ is temperature-dependent and

increases at lower temperatures.[46] According to the AG theory, this implies that the activation free energy of the AA model is greater than that of the CG model (i.e., $\Delta G^{AA} > \Delta G^{CG}$). This also implies that $\Delta G^{CG}(T)$ grows less than $\Delta G^{AA}(T)$ upon cooling, leading to a greater divergence between the AA and CG models at lower temperatures, as one could expect if coarse-graining was greatly influencing s_c of the fluid in relation to the atomistic model. This picture is confirmed from our simulations. Figure 1b shows a comparison of the AA and CG models derived using the IBM method, which involves matching the AA RDF (shown in Figure S1 in the Supporting Information) using tabulated potentials rather than a Lennard-Jones approximation. The comparison reveals a similar increasing trend, but a notable divergence in $\Delta G(T)$ between the AA and CG PS models upon cooling. Here, $\Delta G(T)$ is evaluated from the segmental relaxation data τ_{seg} by calculating the second Legendre order parameter $P_2(t)$ of the bond vector AA (see section 2.3, Simulation Methods). It is then evident that our main difficulty in capturing fluid dynamics is the preservation of ΔG under coarse-graining.

For this purpose, the generalized entropy theory (GET), a combination of the AG model and the lattice cluster theory (LCT) of polymer melts, provides a tractable theoretical framework to develop CG models that capture atomistic dynamics. Specifically, the GET predicts that the strength of the monomeric cohesive interaction, often described by the cohesive interaction parameter ε in the Lennard-Jones (LJ) potential, has a direct influence on the dynamics of GF liquids as manifested by its effects on factors such as s_c, dynamic fragility, and characteristic temperatures of glass formation. This has been verified in recent molecular simulations by Xu et al.,[36,41] where ε was shown to correlate with s_c, activation enthalpy and τ. A large body of evidence has suggested that an “entropy-enthalpy compensation” effect can be expected for polymer fluids wherein entropy and enthalpy of activation vary proportionally as molecular parameters are varied.[30–33]If the compensation effect is operative under coarse-graining, then correcting ε as a function of temperature might allow us to capture the fluid dynamics by preserving the overall $\Delta G(T)$.

Notably, the GET indicates that z(T) for flexible polymers evolves *sigmoidally* with temperature, wherein the CRR size is a constant value in the Arrhenius regime, but grows upon cooling until reaching a plateau value in the non-equilibrium glassy regime.[47,48] Accordingly, since ΔG of both the AA and CG models have similar form but with a different range of variation, it follows that a sigmoidally dependent cohesive interaction term $\varepsilon(T)$ in a CG model (provided that a good approximation of the AA model density is maintained via $\sigma(T)$) might be sufficient to reproduce the full atomistic GF dynamics. We put this idea to the test by introducing a temperature dependent rescaling factor $\alpha(T)$ (i.e., $\varepsilon(T) = \alpha(T)\varepsilon^0$, where ε^0 is the initial cohesive interaction parameter determined by the IBM), which would be required to capture AA dynamics in a chemically specific two-bead CG model for PS. Similarly, the density is preserved by the introduction of $\beta(T)$ (i.e., $\sigma(T) = \beta(T)\sigma^0$, where σ^0 is also obtained by the IBM).

2.2. Coarse-Grained Mapping.

Our findings are built upon molecular dynamics (MD) simulations of a two-bead-permonomer ($\lambda = 8$ atoms per bead on average) CG model for atactic PS by Hsu et al.

(Figure 1a),[40] from which we retrieve the bonded interactions (bond, angle, dihedral potentials) derived by the IBM[4,5] (summarized in Table S1 in the Supporting Information). Here, we focus on parametrizing basic molecular parameters σ and ε for which we adopt the standard 12−6 LJ potential as described above, which is commonly applied for the CG models with the form:

$$U_{nonbond} = 4\varepsilon\left[\left(\frac{\sigma}{r}\right)^{12} - \left(\frac{\sigma}{r}\right)^{6}\right] + S_{LJ}(r) r < r_{\text{outer}} \quad (3)$$

where σ governs the effective van der Waals radius of the CG model and marks the distance at which U_{nonbond} is zero, and ε is the depth of the potential well in energy unit. The polynomial term $S_{LJ}(r)$ is implemented to ensure a smooth transition to zero energy and force from r_{inner} = 12 Å to r_{outer} = 15 Å.[49]

The CG model considers six different parameters for U_{nonbond}: σ_{AA} and ε_{AA} for backbone and backbone (*AA*) interactions, σ_{BB} and ε_{BB} for side-group and side-group (*BB*) interactions, and σ_{AB} and ε_{AB} for backbone and side-group (*AB*) interactions. The cross-interaction terms σ_{AB} and ε_{AB} are taken as the arithmetic $\left(\sigma_{AB} = \frac{1}{2}(\sigma_{AA} + \sigma_{BB})\right)$ and geometric averages $\left(\varepsilon_{AB} = \sqrt{\varepsilon_{AA}\varepsilon_{BB}}\right)$ of the AA and BB terms, respectively. Temperature rescaling factors $\beta(T)$ and $\alpha(T)$ are implemented for σ and ε, respectively. Therefore, the effective LJ parameters σ and ε can be expressed as a function of T by introducing "renormalization factors": $\varepsilon_{ii} = \alpha(T)\varepsilon_{ii}^{0}$ and $\sigma_{ii} = \beta(T)\sigma_{ii}^{0}$, where the subscripts ii denote either AA or BB. As a starting point, ε_{ii}^{0} and σ_{ii}^{0} are the initial estimates of the nonbonded LJ parameters, which can be obtained from the AA radial distribution function (RDF) of the CG force centers: $U^{0}_{\text{nonbond}}(r) = -k_B T \ln[g'(r)]$, where g′(r) is the RDF measured from the AA monomer model as shown in Figure S1 in the Supporting Information.

2.3. Simulation Methods.

All our simulations are carried out using the LAMMPS software package.[50] For the simulations of AA PS, a DREIDING force-field is employed.[51] The chain length N = 10 is used to calculate physical properties and derive CG force-fields − the small N value in this demonstration is chosen due to its computational expediency, but the method should be applicable to other chain lengths. The simulated AA and CG systems consist of 24 300 and 12 140 beads, respectively. Periodic boundary conditions are used in all the directions to simulate bulk properties of PS. A timestep Δt of 1 fs and 4 fs is chosen for the AA and CG simulations, respectively. During the equilibration, the total energy of the system is minimized via the conjugate gradient algorithm, followed by annealing cycle between 210 K and 1000 K for 4 ns, respectively, under the isothermal−isobaric (NPT) ensemble with a constant 101 kPa (1 atm) applied. Then, the systems are further relaxed for 2 ns at 850 K.

For the calculation of self-diffusivity D, we calculate the MSD of the center of mass of polymer chains via the Einstein relation of the form:

$$D = \lim_{t \to \infty} \frac{1}{6t} \left\langle r_{\mathrm{CM}}(t) - r_{\mathrm{CM}}(0)^2 \right\rangle \quad (4)$$

where $r_{\mathrm{CM}}(t)$ is the position of the center of mass of each chain at time t. The segmental relaxation time τ_{seg} is calculated by the second Legendre order parameter $P_2(t)$:

$$P_2(t) = \frac{3}{2} \left\langle \cos^2 \theta(t) \right\rangle - \frac{1}{2} \quad (5)$$

Where $\theta(t)$ is the angle of a vector under consideration at time t relative to its position at $t = 0$. The vector is chosen to be parallel to the backbone vector (i.e., AA bond) of the CG polymer chain, which connects two nonconsecutive carbon atoms separated by one carbon in the corresponding AA system. We then fit $P_2(t)$ with a stretched exponential function: $P_2(t) = \exp\left[-\left(\frac{t}{\tau_{KWW}} \right)^{\beta^{KNW}} \right]$, where τ_{KWW} and β^{KWW} Kohlrausch−Williams−Watts (KWW) parameters that describe relaxation process. The segmental relaxation time τ_{seg} can be determined as the integral of the KWW curves with the expression: $\tau_{seg} = \left(\frac{\tau_{KWW}}{\beta^{kWw}} \right) \Gamma\left(\frac{1}{\beta^{KWN}} \right)$, where Γ() is the gamma function. The shear modulus G is calculated by nonequilibrium MD simple shear simulations at a constant shear strain rate of 0.5 ns^{-1}, from which the shear modulus G can be obtained from the linear slopes in the elastic regime ($\lesssim$ 2% strain). The stress component in the shear deformation is calculated based on the atomic virial stress tensor:[52]

$$\sigma_{xy} = -\frac{1}{V} \left[\sum_{A}^{n} m_A (v_A)_x (v_A)_y + \sum_{A>B}^{n} \frac{\partial U}{\partial r_{AB}} \frac{(r_{AB})_x (r_{AB})_y}{r_{AB}} \right] \quad (6)$$

where V is the volume of the system, n is the total number of CG beads, r_{AB} is the distance between bead pairs A and B, U is the total energy of the system, and m_{A} and v_{A} denote the mass and velocity of the nth bead, respectively.

3. RESULTS

3.1. Capturing Atomistic Dynamics via Energy-Renormalization.

We begin our analysis in the Arrhenius regime where the activation energy remains temperature independent. In this regime, the self-diffusivity D of polymer system can be described by an Arrhenius temperature dependence:[42,43,53] $D(T) = D_0 \exp\left(-\frac{\Delta E}{k_{\mathrm{B}} T} \right)$, where D_0 is a prefactor and ΔE is the activation energy of diffusion. This Arrhenius behavior is limited to a high temperature regime above onset temperature T_{A}, below which the D starts to deviate from the Arrhenius scaling. T_{A} can be estimated from the segmental relaxation data τ_{seg} as

reported in prior work.[33] The calculation of T_A of the AA system is shown in Figure S3 in the Supporting Information.

As noted before, the activation energy of diffusion in the high temperature regime is largely independent of temperature and scales linearly with the cohesive interaction strength (i.e., $\Delta E \sim \varepsilon$).[47] It is well-known that the heat of vaporization also follows a linear scaling with respect to ΔE for many fluids, consistent with their direct relation between ΔE and cohesive interaction.[43,54] We then expect that increasing ε by a single scalar α_A should enable the CG model to capture the ΔE of the AA system.. We test this hypothesis by investigating the effect of α on the D of CG models. The Arrhenius fits in Figure 2a indicate that varying the cohesive interaction strength indeed renormalizes the ΔE of the CG system, which increases linearly with α (inset of Figure 2b). In the Arrhenius regime at high T, the CG model can reproduce D and ΔE of the AA system by a constant value $\alpha_A \approx 2.3$ as shown in Figure 2b.

At lower temperatures, below the onset temperature T_A for non-Arrhenius relaxation, we can expect that a constant renormalization of ε will not provide an adequate description of AA dynamics as the activation energy becomes temperature dependent. Accordingly, in the GF regime, we use atomistic segmental relaxation to determine α in this non-Arrhenius regime. Figure 3a shows the effect of cohesive interactions on τ_{seg} of the CG models with varying α. τ_{seg} increases with α in a nonlinear fashion, which is consistent with recent simulation work.[36] To capture the atomistic τ_{seg} (marked as dashed lines in the plot) in the CG model, we need to renormalize ε at each temperature in this non-Arrhenius regime. The effect of adjusting cohesive energies on the non-Arrhenius relaxation dynamics becomes more pronounced as temperature is lowered toward T_g, as expected from the GET.[47]

By employing a temperature-dependent energy-renormalization scheme, we find a good agreement between the segmental relaxation dynamics of the CG and AA models in this regime, shown in Figure 3b. The temperature dependent τ_{seg} of both AA and CG models can be captured by a single Vogel−Fulcher − Tammann (V F T) expression :[55–57] $\tau_{seg}(T) = \tau_0 \exp\left(\frac{\bar{D}T_0}{T - T_0}\right)$, where $\tau 0$, $\bar{D}$and $T0$ are fitting parameters that characterize the relaxation process. The Vogel temperature T_0 dictates the “end” of glass formation range, where the structural relaxation time formally extrapolates to an infinite value, and $\bar{D}$ is inversely related to the fragility parameter K.[47] The T_0 is estimated to be about 250 K for the AA and CG systems with a chain length $N = 10$ based on the VFT fits. T_g can be determined by extrapolating the relaxation data to the empirical observation time scale, $\tau_{seg}(T_g) \approx 100$ s, which we find to be about 280 K for the AA and CG models. This T_g estimation is in good agreement with the values determined experimentally, after accounting for the molecular mass effect using the Flory−Fox relation ($T_g \approx 273$ K).[58] The dashed slope shows the Arrhenius fit to τ_{seg} for the CG model at high temperatures, and the onset temperature T_A, below which non-Arrhenius relaxation occurs, is estimated to be about 600 K (marked by a vertical dashed line in Figure 3b), consistent with the AA estimate.

We also evaluate another important characteristic temperature of GF processes, the so-called “localization temperature” T_l, which represents the onset of caged particle motion (schematically illustrated in Figure 3c) – a quantity closely related to T_A.[33,59] As discussed

previously, caging effects manifest as local minima of the logarithmic derivative of the segmental mean-squared displacement (MSD) $\left\langle r^2(t)\right\rangle$: $\frac{\partial\left[\ln\left\langle r^2(t)\right\rangle\right]}{\partial[\ln(t)]}$(here,$\langle r^2\rangle$ and t are defined relative to basic atomic length and time scales, 1 Å and 1 fs). As shown in Figure 3c and 3d, by implementing $\alpha(T)$, we observe that both the AA and CG models exhibit caging minima at around 4 ps at lower temperatures until it vanishes at $T_l \approx 560$ K (highlighted by the dashed line in the plots), which is somewhat lower than $T_A \approx 600$ K. It is evident that the CG model is capable of reproducing the characteristic temperatures of glass formation for the AA model.

We proceed to study the dynamics in the non-equilibrium glassy regime ($T \lesssim T_g$) where τ_{seg} becomes intractable. Accordingly, we analyze the high-frequency shear modulus G, an important dynamic and mechanical property that is strongly correlated with the segmental dynamics in the non-equilibrium glassy regime.[60] Figure 4a shows the shear stress vs. strain plot that illustrates the effect of cohesive energy-renormalization on the shear modulus G. Our result demonstrates that both stress response and G of the CG models are strongly dependent on α. As α is varied from 2.8 to 3.7, G increases correspondingly from 0.47 to 0.85 GPa at $T = 250$ K, respectively. The stress−strain curve of the AA model falls in between $\alpha = 3.4$ and 3.7, yielding a G estimate of 0.81 GPa. Similar to the high-T Arrhenius regime where α was chosen to be a constant, using a temperature invariant α ($\alpha_g \approx 3.6$) can reproduce the atomistic G in the glassy regime, as shown in the inset of Figure 4a. The convergence to a constant value agrees well with the expected trends for $z(T)$ and the string (CRR) size,[61] which is predicted to saturate to a finite value at low T. This can also be rationalized by the notion that s_c depends weakly on T in the glassy regime below T_g, due to a near constant residual entropy of the fluid.

Next, we analyze the success of α_g in capturing caging effects in the glassy regime by calculating the Debye−Waller factor (DWF) $\langle u^2\rangle$, a physical quantity related to thermal vibrations of atoms in a glassy solid at picosecond time scales. This quantity can be measured experimentally via incoherent neutron scattering experiments. The DWF is effectively a measure of local molecular stiffness,[62–65] and has been shown to be empirically related to G by an inverse scaling relation of the form[66] $G \approx A + B/\langle u^2\rangle$, where A and B are constants. We define $\langle u^2\rangle$ as the MSD of the center-of-mass of the chain segments for the AA and CG models at the previously defined caging time of around 4 ps. We verify this scaling relationship between G and $1/\langle u^2\rangle$ for our AA and CG model for a range of temperatures in the glassy state (Figure 4b). The quantitative agreement between AA and CG model demonstrates that our coarse-graining approach can accurately reproduce segmental dynamics of the atomistic system even at the non-equilibrium glassy state.

3.2. Energy-Renormalization Covering the Entire Range of Glass Formation.

Strikingly, our analyses confirm our hypothesis that the form of $\alpha(T)$ can be approximated by a sigmoidal function, where it attains constant values in the glassy and Arrhenius regimes with $\alpha g > \alpha A$, and transitions smoothly between these states to compensate for the difference in the AA and CG segmental relaxation dynamics. Figure 5 summarizes this concept by illustrating the complete temperature dependent renormalization function $\alpha(T)$

that scales ε_{ii}^{0} (estimated from the IBM) to match dynamics in the entire range of glass formation:

$$\alpha(T) = \left(\alpha_A - \alpha_g\right)\Phi + \alpha_g \quad (7)$$

where α_g and α_A refer to α values in the glassy and Arrhenius regimes, respectively; Φ is the two-state crossover function taking the form $\Phi = 1/[1 + \exp(-k(T - T_T)]$, where k is a parameter related to the temperature breadth of the transition, and T_T ($\approx$ 475 K) describes the crossover point of this sigmoidal function from the Arrhenius to glassy regimes.

We note that we have also performed a similar rescaling procedure for the other LJ parameter, σ, the length-scale parameter of the molecular interaction. This quantity is an important molecular parameter that influences the thermodynamics of the fluid. Since σ is also directly related to the density, this quantity can readily be renormalized to bring the AA and CG densities into alignment. In particular, the corresponding temperature renormalization factor $\beta(T)$ is derived by demanding the AA density at different temperatures to be consistent with the CG model (see Figure S3 in the Supporting Information). We find that the derived $\beta(T)$ takes the linear form $\beta(T) = aT + b$, where a and b are constants, leading to an excellent agreement between AA and CG densities over a wide temperature range as shown in Figure 6. While our main focus is on the renormalization of the cohesive interaction strength parameter ε due to its primary influence on the fluid dynamics, σ and density are clearly important factors in influencing the dynamics of the glass-forming systems. [67–69] The functional forms and parameters of $\alpha(T)$ and $\beta(T)$ are summarized in Table S2 in the Supporting Information. With the derived $\alpha(T)$ and $\beta(T)$, we find that we can successfully preserve the density and recover both the shorter time (i.e., DWF) and longer time dynamics (i.e., diffusivity and segmental relaxation). This is also demonstrated by the quantitative agreement of the MSD of chain segments between AA and CG models (inset in Figure 5). Therefore, our renormalization approach corrects all the usual shortcomings of state-point derived CG models (i.e., faster dynamics, softer mechanical response and a lack of temperature transferability).

4. DISCUSSION

As mentioned above, the sigmoidal variation of $\alpha(T)$ can be understood from the alteration of $z(T)$, the collective motion (CRR) size in the AG theory and its generalization form, GET. The GET predicts that $z(T)$ for flexible polymer grows upon cooling and saturates to a finite value in the low-T glassy regime, where we interpret the saturation of $\alpha(T)$ to reflect this effect.[47,48] Many features of the AG theory and GET have been confirmed by recent molecular dynamics studies of GF liquids.[36] On the basis of this simulation evidence, a "string" model of glass formation has been recently proposed,[61] which quantifies $z(T)$ in terms of the average polymerization index of cooperative string-like clusters of rearranging particles. The GET is consistent with these predictions and further predicts a sigmoidal variation of $z(T)$ with temperature, which has since been verified in various GF system. We note, however, that $z(T)$ should not be equated to $\alpha(T)$, which is instead a measure of how

much coarse-graining alters the configurational entropy s_c of the fluid and the consequences of these changes on collective motion in the cooled liquid.[33,36,59]

The sigmoidal nature of $\alpha(T)$ in our work provides supporting evidence that the activation energies of polymers should exhibit saturation upon reaching the glassy limit,[70] a finding consistent with the string model of cooperative motion, as well as the GET of flexible polymers. On the basis of these findings, the next step would be to directly characterize the string lengths and s_c of the AA and CG models, respectively, to precisely quantify the differences in $\Delta G(T)$ in cooled regimes, and provide a direct way to determine $\alpha(T)$, which we plan to study in our future work. Moreover, it might be also possible to calculate $\alpha(T)$ analytically from the GET based on the findings that $s_c(T)$ is greatly altered by the cohesive interaction.[48]

In addition, the CG model via energy-renormalization allows for the prediction of the characteristic temperatures of glass formation (T_A, T_l, T_g, T_0). This is done by comparing key ratios of the AA and CG characteristic temperatures, and considering the GET predictions for a polymer with flexible backbones and stiff side chains (F−S),[47] which are all listed in Table S3 in the Supporting Information. As expected, the calibrated CG model has nearly identical characteristic temperature ratios as the AA model. The GET prediction follows a similar trend, but has slightly lower magnitudes, which could be attributed to the idealization of monomeric structure in the GET.[47] The two characteristic temperatures T_g and T_A, which mark the transition points from the glassy regime to the non-Arrhenius regime, and the non-Arrhenius regime to the Arrhenius regime, respectively, are identified in Figure 5. There is a good correlation between these temperatures and the onset of plateaus in $\alpha(T)$. We also note that T_T, which is the empirical transition point in our $\alpha(T)$ function, resides between T_A and T_g, which confirms that the degree of the temperaturedependent renormalization needed for the cohesive interaction parameter is related to the dynamics of glass formation. The scaling functional form of $\alpha(T)$ and its correlation with the characteristic temperatures identified through our study could be further utilized to quickly estimate the cohesive interaction strength with fewer state-point calculations.

With this method in mind, we hypothesize that we may develop general CG models for different classes of GF materials. For instance, we may hypothesize that a more fragile GF material should exhibit a larger α, as it will likely have a larger CRR size,[71] and thus a larger temperature-dependent activation energy upon cooling. By the same logic, a less fragile GF material would exhibit a smaller α, and eventually flatten out for a completely Arrhenius glass-former (i.e., extremely “strong” GF liquid). Second, we can expect that increasing degree of coarse-graining λ (i.e., the number atoms per CG bead) should naturally cause greater loss in configurational entropy and therefore accelerate chain dynamics.[72] This effect should become enhanced toward lower temperatures where the deviation between AA and CG configurational entropies grows more rapidly for high λ, and thus we can anticipate α to be directly related to λ. Understanding and validating these effects in future work will be important in establishing more comprehensive CG modeling approaches for a wide range of GF materials − not only polymers, but also biopolymers, metallic glasses, and small molecule liquids that exhibit cooperative dynamics upon amorphous solidification.

There are a few other future topics that are worth exploring to improve our CG methodology. First, while the CG model is able to recover atomistic dynamics and thermodynamic properties, such as density, over an impressive range of temperature, this comes at the cost of accurately reproducing the local structure of the atomistic chains (i.e., RDF). As shown in Figure S4 in the Supporting Information, our CG model only captures qualitative characteristics of the AA RDF (e.g. the first peak location in the RDF). The magnitude of the first peak is consistently higher for the CG model, which is perturbed by the shift of the nonbonded potential. Similar observations have also been reported in the past,[15,40] although we note that our CG modeling method seems to yield RDFs that are more consistent with AA data than prior efforts that aimed to reproduce dynamics through similar means. Accordingly, capturing structure, dynamics, and transferability within a single CG model remains an elusive goal, warranting further investigations. It would also be interesting to explore the effect of imposing a temperature-dependent frictional and dissipative factors in methods such as DPD,[25] based on the idealizations of Mori and Zwanzig.[18] Since those frictional terms are functionally performing a similar role in modulating the dynamics of the system, we may expect that the state-point dependent scaling of frictional terms result in a similar outcome to the findings of the present work, although the ability to replicate dynamics in the glassy regime relevant to polymer applications via such methods remains an open question. While our proposed energy-renormalization approach is based on a classic molecular dynamics rather than a Langevin type molecular dynamics, combining our approach with a Langevin treatment might provide an alternative route toward establishing an efficient CG modeling framework that captures both dynamic and thermodynamic properties in the CG model. This would also be an interesting topic for a future study.

5. CONCLUSION

We have established an energy-renormalization scheme for achieving temperature transferable CG modeling of polymer materials. In light of the AG theory of glass formation, we show that renormalizing the cohesive interaction strength and effective interaction length-scale parameters under coarsegraining as a function of temperature allows for the “correction” of many of the usual shortcomings of state-point derived CG models (i.e., faster dynamics, softer mechanical response and a lack of temperature transferability). Strikingly, we find that the derived energy-renormalization factor $\alpha(T)$ in the cohesive interaction replicates the sigmoidal functional form of the activation free energy, as predicted by the GET and the recent string model. These findings shed light on not only developing effective temperature transferable models for GF systems, but also on the fundamental effects of reduced-order modeling and its impact on GF dynamics as predicted by GF theories. As our work essentially entails the direct validation of theoretical predictions of GF phenomena as functions of molecular parameters, we expect our approach to be general for GF systems beyond polymeric materials, and to stimulate many future studies on developing state-point transferable computational models for the rational design of materials.

Supplementary Material

Refer to Web version on PubMed Central for supplementary material.

ACKNOWLEDGMENTS

The authors acknowledge support by the National Institute of Standards and Technology (NIST) through the Center for Hierarchical Materials Design (CHiMaD). W.X, J.S., D.D.H, and S.K. acknowledge support from the Department of Civil & Environmental Engineering, Mechanical Engineering and Materials Science and Engineering at Northwestern University. W.X. gratefully acknowledges the support from the NISTCHiMaD Postdoctoral Fellowship. S.K. acknowledges support from an ONR Director of Research Early Career Award (PECASE, Award #N00014163175). A supercomputing grant from Quest HPC System at Northwestern University is acknowledged.

REFERENCES

(1). Debenedetti PG; Stillinger FH Supercooled liquids and the glass transition. Nature 2001, 410 (6825), 259–267. [PubMed: 11258381]

(2). Hedler A; Klaumunzer SL; Wesch W Amorphous silicon exhibits a glass transition. *Nat.* Mater. 2004, 3 (11), 804–809. [PubMed: 15502833]

(3). van der Sman RGM Predictions of Glass Transition Temperature for Hydrogen Bonding Biomaterials. J. Phys. Chem. B 2013, 117 (50), 16303–16313. [PubMed: 24308288]

(4). Müller-Plathe F Coarse-graining in polymer simulation: from the atomistic to the mesoscopic scale and back. ChemPhysChem 2002, 3 (9), 754–769.

(5). Reith D; Putz M; Muller-Plathe F Deriving effective mesoscale potentials from atomistic simulations. *J. Comput. Chem*. 2003, 24 (13), 1624–36. [PubMed: 12926006]

(6). Fritz D; Koschke K; Harmandaris VA; van der Vegt NFA; Kremer K Multiscale modeling of soft matter: scaling of dynamics. *Phys. Chem. Chem. Phys*. 2011, 13 (22), 10412–10420. [PubMed: 21468407]

(7). Karimi-Varzaneh HA; van der Vegt NFA; Müller-Plathe F; Carbone P How Good Are Coarse-Grained Polymer Models? A Comparison for Atactic Polystyrene. ChemPhysChem 2012, 13 (15), 3428–3439. [PubMed: 22714871]

(8). Lyubartsev AP; Laaksonen A Calculation of Effective Interaction Potentials from Radial-Distribution Functions - a Reverse Monte-Carlo Approach. *Phys. Rev. E: Stat. Phys., Plasmas, Fluids, Relat. Interdiscip.* Top. 1995, 52 (4), 3730–3737.

(9). Izvekov S; Voth GA A multiscale coarse-graining method for biomolecular systems. *J. Phys. Chem.* B 2005, 109 (7), 2469–2473. [PubMed: 16851243]

(10). Izvekov S; Voth GA Multiscale coarse graining of liquid-state systems. *J. Chem. Phys*. 2005, 123 (13), 134105. [PubMed: 16223273]

(11). Noid WG; Chu JW; Ayton GS; Krishna V; Izvekov S; Voth GA; Das A; Andersen HC The multiscale coarse-graining method. I. A rigorous bridge between atomistic and coarse-grained models. *J. Chem. Phys*. 2008, 128 (24), 244114. [PubMed: 18601324]

(12). Noid WG; Liu P; Wang Y; Chu JW; Ayton GS; Izvekov S; Andersen HC; Voth GA The multiscale coarsegraining method. II. Numerical implementation for coarse-grained molecular models. *J. Chem. Phys*. 2008, 128 (24), 244115. [PubMed: 18601325]

(13). Shell MS The relative entropy is fundamental to multiscale and inverse thermodynamic problems. *J. Chem. Phys*. 2008, 129 (14), 144108. [PubMed: 19045135]

(14). Shell MS Coarse-Graining with the Relative Entropy. Advances in Chemical Physics 2016, 395–441.

(15). Rosch TW; Brennan JK; Izvekov S; Andzelm JW Exploring the ability of a multiscale coarse-grained potential to describe the stress-strain response of glassy polystyrene. Phys. Rev. E 2013, 87 (4), 042606.

(16). Grmela M; Ö ttinger HC Dynamics and thermodynamics of complex fluids. I. Development of a general formalism. *Phys. Rev. E: Stat. Phys., Plasmas, Fluids, Relat. Interdiscip. Top*. 1997, 56 (6), 6620–6632.

(17). Ö ttinger HC; Grmela M Dynamics and thermodynamics of complex fluids. II. Illustrations of a general formalism. *Phys. Rev. E: Stat. Phys., Plasmas, Fluids, Relat. Interdiscip. Top*. 1997, 56 (6), 6633–6655.

(18). Hijon C; Espanol P; Vanden-Eijnden E; Delgado-Buscalioni R Mori-Zwanzig formalism as a practical computational tool. Faraday Discuss. 2010, 144, 301–322. [PubMed: 20158036]

(19). Zwanzig R Nonlinear generalized Langevin equations. *J. Stat. Phys*. 1973, 9 (3), 215–220.

(20). Adam G; Gibbs JH On the temperature dependence of cooperative relaxation properties in glass-forming liquids. *J. Chem. Phys*. 1965, 43 (1), 139–146.

(21). Adelman SA; Balk MW Generalized Langevin theory for many-body problems in chemical dynamics: The equivalent chain equations for solute motion in molecular solvents. J. Chem. Phys 1986, 84 (3), 1752–1761.

(22). Groot RD; Warren PB Dissipative particle dynamics: Bridging the gap between atomistic and mesoscopic simulation. *J. Chem. Phys*. 1997, 107 (11), 4423–4435.

(23). Español P; Serrano M; Zuñiga I Coarse-Graining of a Fluid and its Relation with Dissipative Particle Dynamics and Smoothed Particle Dynamic. International Journal of Modern Physics C 1997, 08 (04), 899–908.

(24). Qian H-J; Liew CC; Muller-Plathe F Effective control of the transport coefficients of a coarse-grained liquid and polymer models using the dissipative particle dynamics and Lowe-Andersen equations of motion. *Phys. Chem. Chem. Phys*. 2009, 11 (12), 1962–1969. [PubMed: 19280007]

(25). Español P; Warren PB Perspective: Dissipative particle dynamics. *J. Chem. Phys*. 2017, 146 (15), 150901. [PubMed: 28433024]

(26). Espanol P; Zuniga I Obtaining fully dynamic coarse-grained models from MD. *Phys. Chem. Chem. Phys*. 2011, 13 (22), 10538–10545. [PubMed: 21442096]

(27). Davtyan A; Dama JF; Voth GA; Andersen HC Dynamic force matching: A method for constructing dynamical coarse-grained models with realistic time dependence. *J. Chem.* Phys. 2015, 142 (15), 154104. [PubMed: 25903863]

(28). Davtyan A; Voth GA; Andersen HC Dynamic force matching: Construction of dynamic coarse-grained models with realistic short time dynamics and accurate long time dynamics. *J. Chem. Phys*. 2016, 145 (22), 224107. [PubMed: 27984910]

(29). Noid WG Perspective: Coarse-grained models for biomolecular systems. *J. Chem. Phys*. 2013, 139 (9), 090901. [PubMed: 24028092]

(30). Yelon A; Movaghar B Microscopic explanation of the compensation (Meyer-Neldel) rule. *Phys. Rev.* Lett. 1990, 65 (5), 618–620. [PubMed: 10042969]

(31). Yelon A; Movaghar B; Crandall RS Multi-excitation entropy: its role in thermodynamics and kinetics. *Rep. Prog. Phys*. 2006, 69 (4), 1145.

(32). Jeong C; Douglas JF Mass dependence of the activation enthalpy and entropy of unentangled linear alkane chains. *J. Chem. Phys*. 2015, 143 (14), 144905. [PubMed: 26472396]

(33). Pazmiño Betancourt BAP; Hanakata PZ; Starr FW; Douglas JF Quantitative relations between cooperative motion, emergent elasticity, and free volume in model glass-forming polymer materials. *Proc. Natl. Acad. Sci. U. S.* A. 2015, 112 (10), 2966–2971. [PubMed: 25713371]

(34). Lumry R; Rajender S Enthalpy−entropy compensation phenomena in water solutions of proteins and small molecules: A ubiquitous properly of water. Biopolymers 1970, 9 (10), 1125–1227. [PubMed: 4918636]

(35). Krug RR; Hunter WG; Grieger RA Statistical interpretation of enthalpy-entropy compensation. *Natur*e 1976, 261 (5561), 566–567.

(36). Xu W-S; Douglas JF; Freed KF Influence of Cohesive Energy on Relaxation in a Model Glass-Forming Polymer Melt. Macromolecules 2016, 49 (21), 8355–8370.

(37). Cao F; Sun H Transferability and Nonbond Functional Form of Coarse Grained Force Field − Tested on Linear Alkanes. J. Chem. Theory Comput 2015, 11 (10), 4760–4769. [PubMed: 26574265]

(38). Xia W; Mishra S; Keten S Substrate vs. free surface: Competing effects on the glass transition of polymer thin films. Polymer 2013, 54 (21), 5942–5951.

(39). Hsu DD; Xia W; Arturo SG; Keten S Systematic Method for Thermomechanically Consistent Coarse-Graining: A Universal Model for Methacrylate-Based Polymers. *J. Chem. Theory Comput*. 2014, 10 (6), 2514–2527. [PubMed: 26580772]

(40). Hsu DD; Xia W; Arturo SG; Keten S Thermomechanically Consistent and Temperature Transferable Coarse-Graining of Atactic Polystyrene. Macromolecules 2015, 48 (9), 3057–3068.

(41). Xu W-S; Freed KF Influence of Cohesive Energy and Chain Stiffness on Polymer Glass Formation. Macromolecules 2014, 47 (19), 6990–6997.

(42). Eyring H Viscosity, Plasticity, and Diffusion as Examples of Absolute Reaction Rates. *J. Chem. Phys*. 1936, 4 (4), 283–291.

(43). Kauzmann W; Eyring H The viscous flow of large molecules. *J. Am. Chem. Soc*. 1940, 62, 3113–3125.

(44). Starr FW; Douglas JF Modifying Fragility and Collective Motion in Polymer Melts with Nanoparticles. *Phys. Rev. Lett*. 2011, 106 (11), 115702. [PubMed: 21469879]

(45). Hanakata PZ; Douglas JF; Starr FW Local variation of fragility and glass transition temperature of ultra-thin supported polymer films. *J. Chem. Phys*. 2012, 137 (24), 244901. [PubMed: 23277950]

(46). Rossi G; Monticelli L; Puisto SR; Vattulainen I; AlaNissila T Coarse-graining polymers with the MARTINI force-field: polystyrene as a benchmark case. Soft Matter 2011, 7 (2), 698–708.

(47). Dudowicz J; Freed KF; Douglas JF Generalized Entropy Theory of Polymer Glass Formation. Advances in Chemical Physics 2008, 125–222.

(48). Xu W-S; Douglas JF; Freed KF Generalized entropy theory of glass-formation in fully flexible polymer melts. *J. Chem. Phys*. 2016, 145 (23), 234509. [PubMed: 28010099]

(49). Lindahl E; Hess B; van der Spoel D GROMACS 3.0: a package for molecular simulation and trajectory analysis. *J. Mol. Model*. 2001, 7 (8), 306–317.

(50). Plimpton S Fast Parallel Algorithms for Short-Range Molecular Dynamics. *J. Comput. Phys*. 1995, 117 (1), 1–19.

(51). Mayo SL; Olafson BD; Goddard WA Dreiding - a Generic Force-Field for Molecular Simulations. *J. Phys. Chem*. 1990, 94 (26), 8897–8909.

(52). Heyes DM Pressure tensor of partial-charge and point-dipole lattices with bulk and surface geometries. *Phys. Rev. B: Condens*. Matter Mater. Phys. 1994, 49 (2), 755–764.

(53). Ewell RH The Reaction Rate Theory of Viscosity and Some of its Applications. *J. Appl. Phys*. 1938, 9 (4), 252–269.

(54). Eirich F; Simha R A Contribution to the Theory of Viscous Flow Reactions for Chain-Like Molecular Substances. *J. Chem. Phys*. 1939, 7 (2), 116–121.

(55). Vogel H The temperature dependence law of the viscosity of fluids. *Phys.* Z. 1921, 22, 645–646.

(56). Fulcher GS Analysis of recent measurements of the viscosity of glasses. *J. Am. Ceram. Soc*. 1925, 8 (6), 339–355.

(57). Tammann G; Hesse W Die Abhängigkeit der Viscosity von der Temperatur bie unterkühlten Flüssigkeiten. Zeitschrift für anorganische und allgemeine Chemie 1926, 156 (1), 245–257.

(58). Fox TG; Flory PJ The Glass Temperature and Related Properties of Polystyrene - Influence of Molecular Weight. *J. Polym. Sci*. 1954, 14 (75), 315–319.

(59). Hanakata PZ; Douglas JF; Starr FW Interfacial mobility scale determines the scale of collective motion and relaxation rate in polymer films. *Nat. Commun*. 2014, 5, 4163. [PubMed: 24932594]

(60). Puosi F; Leporini D Communication: Correlation of the instantaneous and the intermediate-time elasticity with the structural relaxation in glassforming systems. *J. Chem. Phys*. 2012, 136 (4), 041104. [PubMed: 22299854]

(61). Pazmiño Betancourt BA; Douglas JF; Starr FW String model for the dynamics of glass-forming liquids. *J. Chem.* Phys. 2014, 140 (20), 204509. [PubMed: 24880303]

(62). Chung PC; Glynos E; Green PF The Elastic Mechanical Response of Supported Thin Polymer Films. Langmuir 2014, 30 (50), 15200–15205. [PubMed: 25470203]

(63). Xia W; Song J; Hsu DD; Keten S Understanding the Interfacial Mechanical Response of Nanoscale Polymer Thin Films via Nanoindentation. Macromolecules 2016, 49 (10), 3810–3817.

(64). Ye C; Wiener CG; Tyagi M; Uhrig D; Orski SV; Soles CL; Vogt BD; Simmons DS Understanding the Decreased Segmental Dynamics of Supported Thin Polymer Films Reported by Incoherent Neutron Scattering. Macromolecules 2015, 48 (3), 801–808.

(65). Xia W; Keten S Interfacial stiffening of polymer thin film under nanoconfinement. *Extreme Mech. Lett.* 2015, 4, 89–95.

(66). Douglas JF; Pazmino Betancourt BA; Tong X; Zhang H Localization model description of diffusion and structural relaxation in glass-forming Cu−Zr alloys. J. Stat. Mech.: Theory Exp 2016, 2016 (5), 054048.

(67). Bernini S; Puosi F; Leporini D Thermodynamic scaling of relaxation: insights from anharmonic elasticity. *J. Phys.: Condens. Matter* 2017, 29 (13), 135101. [PubMed: 28102828]

(68). Puosi F; Chulkin O; Bernini S; Capaccioli S; Leporini D Thermodynamic scaling of vibrational dynamics and relaxation. *J. Chem. Phys.* 2016, 145 (23), 234904. [PubMed: 27984865]

(69). Xia WJ; Song J; Hsu DD; Keten S Side-group size effects on interfaces and glass formation in supported polymer thin films. *J. Chem. Phys.* 2017, 146 (20), 203311. [PubMed: 28571359]

(70). Zhao J; Simon SL; McKenna GB Using 20-million-yearold amber to test the super-Arrhenius behaviour of glass-forming systems. *Nat. Commun.* 2013, 4, 1783. [PubMed: 23653195]

(71). Saiter A; Saiter JM; Grenet J Cooperative rearranging regions in polymeric materials: Relationship with the fragility of glassforming liquids. *Eur. Polym. J.* 2006, 42 (1), 213–219.

(72). Salerno KM; Agrawal A; Perahia D; Grest GS Resolving Dynamic Properties of Polymers through Coarse-Grained Computational Studies. *Phys. Rev. Lett.* 2016, 116 (5), 058302. [PubMed: 26894738]

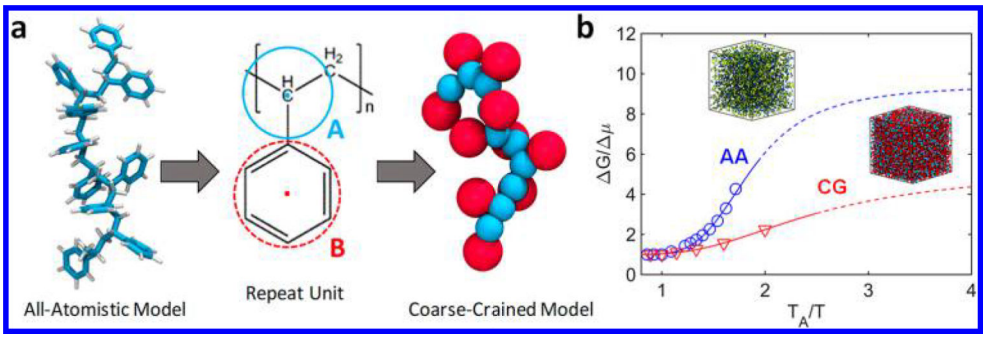

Figure 1.

(a) Coarse-grained model of PS, showing the mapping from (left) all-atomistic (AA) model to (right) coarse-grained (CG) model. (Middle) For each repeat unit, backbone type "*A*" CG bead is centered on the alkyl carbon bonded to phenyl ring. Side-group type "B" CG bead is located at the center of mass of the phenyl ring. (b) Divergence of temperature dependent relative activation energy $\Delta G/\Delta\mu$ for the AA and CG systems (with CG potential derived from the inversed Boltzmann method (IBM) by preserving the AA RDF). The solid and dashed lines illustrate the sigmoidal variation of the activation energy at higher and lower temperatures expected from the GET and AG theory.

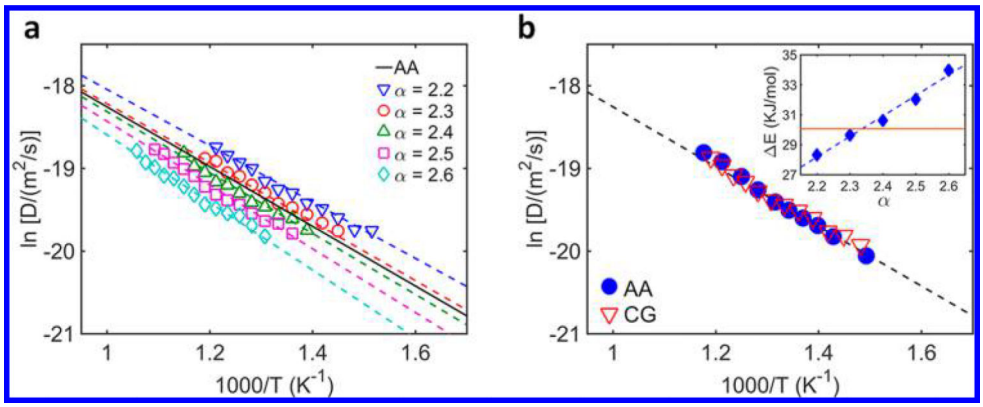

Figure 2.

(a) Self-diffusion coefficients D for AA (solid line) and CG (open symbols) models with varying α parameters in the high temperature regime. (b) Comparison of D vs. T for AA and CG models. (Inset) Activation energy of diffusion ΔE as a function of α, which is determined from the Arrhenius fits for each data set in the high temperature regime. The horizontal line shows the ΔE of the AA system.

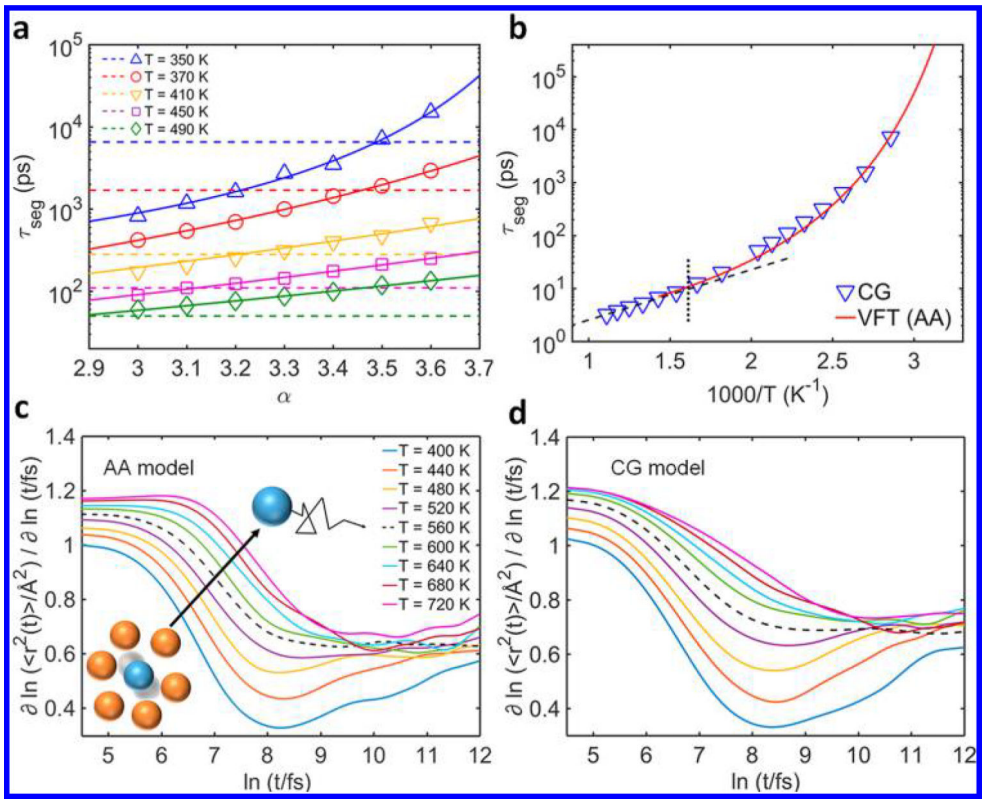

Figure 3.

(a) Segmental relaxation time τseg for AA (dashed lines) and CG (open symbols) models as a function of α. The solid lines are used to show the trend. (b) τseg as a function of temperature for the CG model. The solid curves show the VFT fit of the data for AA model. The dashed slope shows the Arrhenius fit of τseg at high temperatures. The vertical dotted line indicates T_A. Logarithmic derivative of the mean-squared displacement $\partial\left[\ln\left\langle r^2(t)\right\rangle\right]/\partial[\ln(t)]$ as a function of ln(t) for (c) AA and (d) CG models. The dashed lines highlight the localization temperature Tl, representing the onset of caged particle motion. The color legend for different temperatures in (c) is also applied for CG model result in (d). The schematic image in (c) illustrates the transition from particle “caging” dynamics to diffusion dynamics as temperature increases.

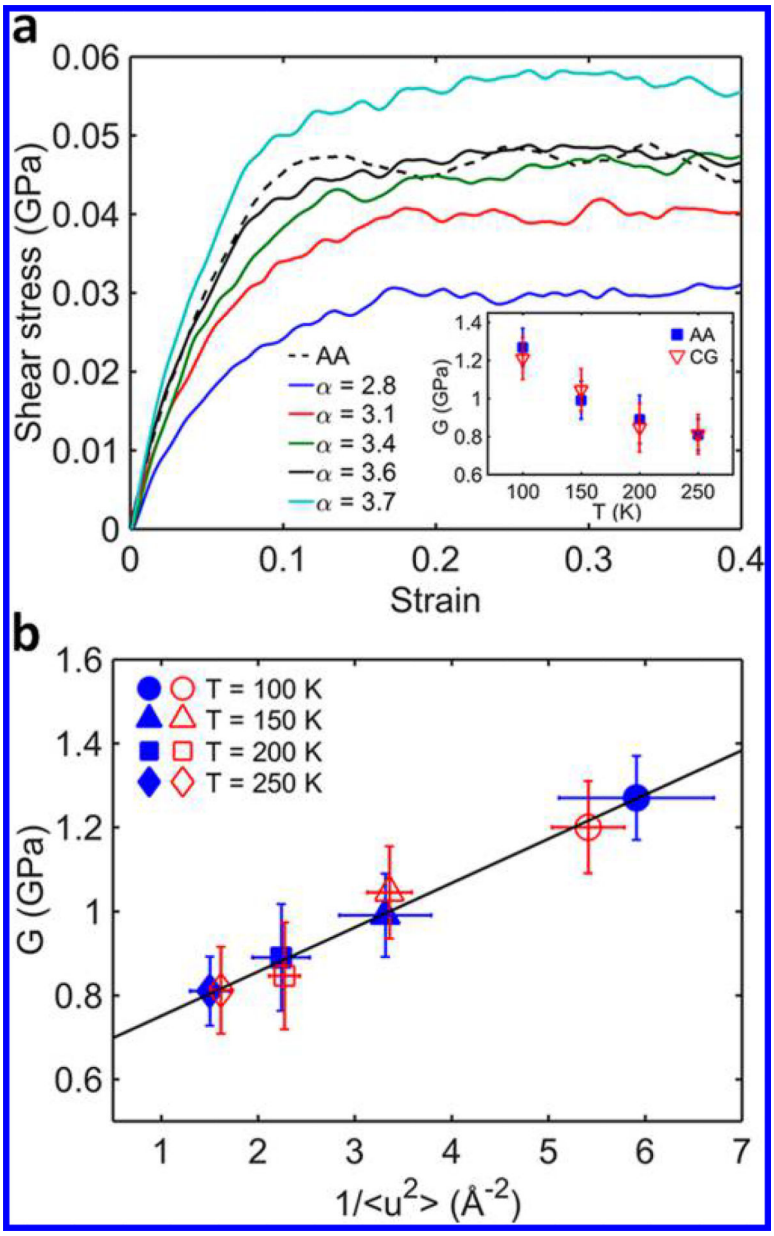

Figure 4.

(a) Shear stress vs. strain curves for the AA model (dotted line) and CG models (solid lines) with varying α at T = 250 K. (Inset) Comparison of shear modulus G at lower temperatures (i.e., nonequilibrium glassy regime) for AA and CG models. (b) Shear modulus G against inversed DWF ($1/\langle u^2 \rangle$) 2 for the AA (filled symbols) and CG model (open symbols) at lower temperatures.

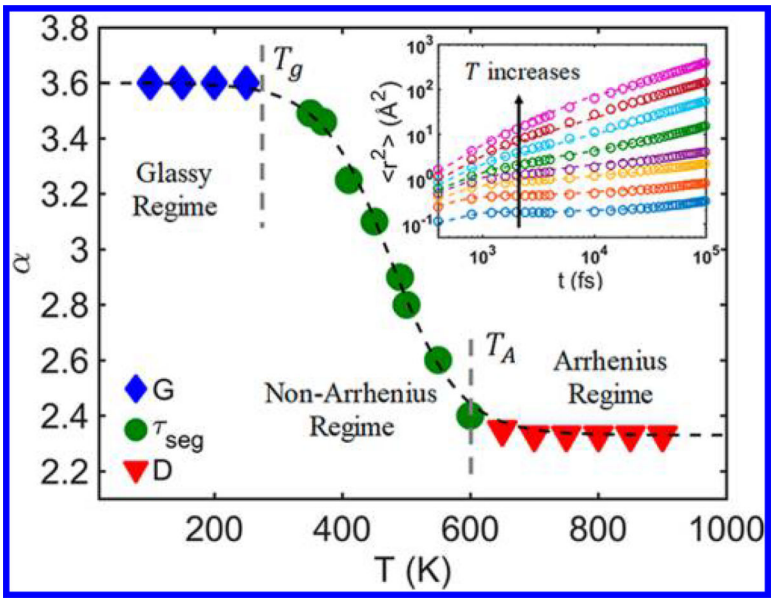

Figure 5.

Temperature-dependent energy-renormalization factor α(*T*) for the CG model. The α(*T*) is obtained by matching the self-diffusion coefficient D, the segmental relaxation time τseg and the shear modulus G of AA model spanning over different temperature regimes (i.e., the Arrhenius, non-Arrhenius, and glassy regimes). (Inset) Comparison of segmental mean-squared displacement vs. time for AA (dashed lines) and CG (open symbols) models at representative temperatures ranging from 100 K to 800 K.

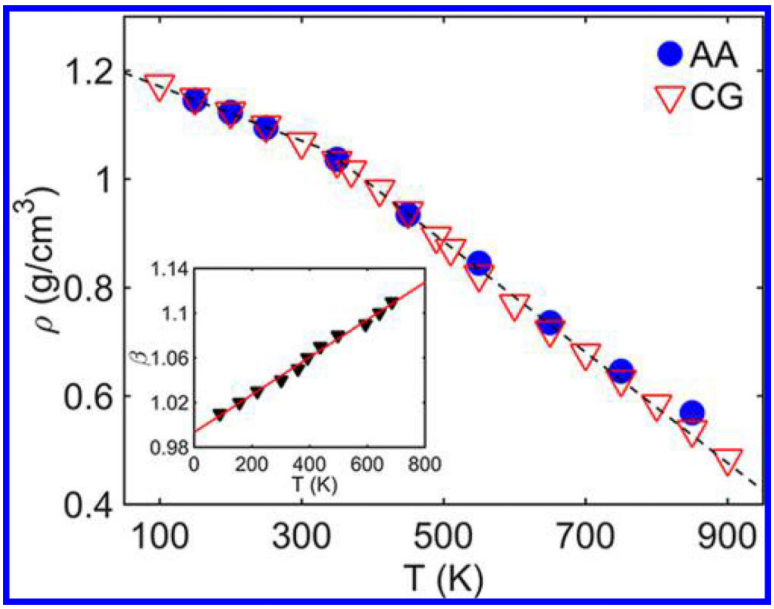

Figure 6.

Comparison of the density ρ as a function of temperature for the AA and CG models. The AA ρ is preserved by the CG model through the renormalization factor $\beta(T)$ for the length-scale parameter σ in the nonbonded cohesive interaction. (Inset) Temperature dependent renormalization factor $\beta(T)$ for the CG model.